

# Optical Properties and Quantum Yield Determination in Photocatalytic Suspensions

V. Loddo, M. Addamo, V. Augugliaro, L. Palmisano, and M. Schiavello

Dipartimento di Ingegneria Chimica dei Processi e dei Materiali, Università di Palermo, 90128 Palermo, Italy

E. Garrone

Dipartimento di Scienza dei Materiali ed Ingegneria Chimica, I Facoltà di Ingegneria, Politecnico di Torino, 10129 Torino, Italy

DOI 10.1002/aic.10883

Published online April 21, 2006 in Wiley InterScience (www.interscience.wiley.com).

*Knowledge of the optical properties of photocatalytic suspensions is vital for a correct comparison of their energetic efficiency. In this work, the determination of both absorption and scattering coefficients of aqueous suspensions of commercial TiO<sub>2</sub> powders irradiated by monochromatic light was carried out by measuring only one quantity—the transmitted photon flow—as a function of the catalyst mass and by applying an asymptotic form of the Kubelka–Munk solution of the radiative transfer equation. Applying a nonlinear fitting procedure the evaluation of the actual values of absorption and scattering coefficients was carried out. The limit for optically thick media of the Kubelka–Munk equation is shown to assume the form of a standard Lambert–Beer absorption formula. The determination of absorbed photon flow was then used to determine the quantum yield value for the phenol photocatalytic oxidation reaction. © 2006 American Institute of Chemical Engineers AIChE J, 52: 2565–2574, 2006*

**Keywords:** heterogeneous photocatalytic reaction, photon absorption, scattering coefficient, absorption coefficient, quantum yield

## Introduction

Remediation of contaminated water is a field of extensive basic and applied research, aimed at developing processes able to destroy very stable inorganic and organic contaminants. Among the advanced oxidation processes developed in the last decades, heterogeneous photocatalysis has been the focus of increasing interest.<sup>1–3</sup>

A photocatalytic system for wastewater treatment generally consists of semiconductor catalyst particles suspended in aqueous solution containing the contaminant species and irradiated by monochromatic or polychromatic light with energy equal to or higher than the band gap. Particles of titanium oxide (TiO<sub>2</sub>) in the anatase phase (band-gap energy  $E_g = 3.2$  eV, corre-

sponding to 382 nm light) are commonly used because of their high photostability, efficiency, and low cost. A very favorable feature of TiO<sub>2</sub> is that the holes photogenerated in the anatase valence band have a sufficiently high positive potential [+2.9 V vs. standard hydrogen electrode (SHE), pH = 0] to oxidize most organic and inorganic compounds to carbon dioxide, water, and mineral acids.

The basic principles of these redox processes have been firmly established, although the search for applications of this technology is just at the beginning stages. Progress in this field is also hampered by the lack of agreement among researchers on the definition of the parameters needed for correctly comparing different photocatalytic systems.<sup>4–8</sup>

Determination of the photon absorption rate in slurry photocatalytic reactors is to date an open question.<sup>9</sup> Indeed, the radiant energy entering a photocatalytic reactor is generally less (sometimes far less) than that impinging on the reacting system, this difference arising from the small catalyst particles

Correspondence concerning this article should be addressed to V. Loddo at loddo@dicpm.unipa.it.

suspended in the liquid phase, which cause scattering and absorption phenomena. The nature of the catalyst powders therefore plays an essential role in determining the radiant field inside the photoreactor. For these systems the radiative transfer is a particular case of radiation transfer within a participating medium,<sup>10</sup> whose optical properties are quantitatively characterized<sup>11</sup> by two parameters: (1) the absorption and scattering coefficients and (2) the phase function for scattering.

The kinetics of photocatalytic reactions is influenced in a complex way both by the concentrations of reactants and products and by the distribution of the radiant field inside the system.<sup>9</sup> The mathematical modeling of the kinetics of photocatalytic reactions requires solution of the problem of radiation transport<sup>12-14</sup> in a medium in which absorption and scattering phenomena occur simultaneously. In principle the effects of radiation absorption and scattering are considered in the solution of the *radiation transfer equation* (RTE). The solution of this governing equation has been carried out using numerical methods based on Monte Carlo simulations<sup>15,16</sup> and also by means of the discrete ordinate method<sup>17-20</sup> (DOM), as used in the field of radiative heat transfer.<sup>21</sup>

The drawback of these methods is that it is necessary to carry out two independent measurements<sup>10</sup> to obtain separate values of the absorption and scattering coefficients: moreover, they require much computer time and do not provide analytical solutions.

It is therefore desirable to develop manageable approximate solutions to the problem of radiation transfer. The most usual approximations made in heterogeneous photocatalysis investigations are either: (1) that all incident radiation is absorbed by the suspension or (2) that a simple expression of the kind of Lambert–Beer law (LBL) describes the radiation field intensity within the suspension.<sup>22</sup> The former approach is far from the experimental conditions adopted in many instances, and in particular in our laboratory, where, following the latter approximation, the optical characterization of suspensions of semiconductor oxides is indeed carried out by measuring the incident and transmitted photon flows.<sup>23-27</sup> In this approach, the suspension was mainly characterized in the past by means of a single phenomenological parameter, the Napierian extinction coefficient,<sup>28</sup> as defined by LBL, suitable for comparing results obtained with the same system at different operative conditions.

A closer inspection of the data suggests, however, that in many instances, two parameters are required to fully characterize the experimental data. For instance, a phenomenological relationship of the LBL kind with two adjustable parameters may be fitted.

We show in the present paper that to the same data the hyperbolic solution of RTE obtained by Kubelka and Munk may be applied, which yields the values of both absorption and scattering coefficients still by determining only one quantity: the transmittance of the suspension as a function of the mass of the catalyst. We further show that an approximated form of the Kubelka–Munk equation for optically thick media assumes the same form of the phenomenological, LBL-like, relationship, with two adjustable parameters, from which the optical coefficients may be readily calculated.

This new approach has been applied to determine the optical properties of some commercial polycrystalline TiO<sub>2</sub> catalysts suspended in water and irradiated by monochromatic radiation.

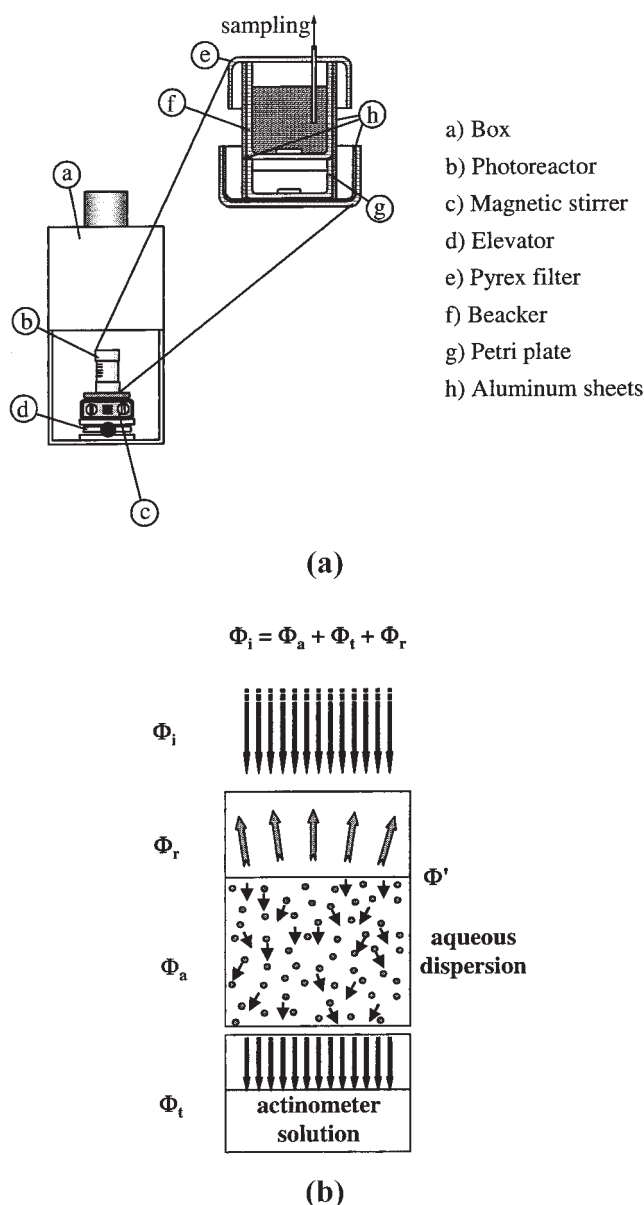


**Figure 1. (a) Experimental setup; (b) scheme of photon balance on photoreactor.**

The evaluation of the radiation field inside the suspension has been applied to the determination of the quantum yield of a photoreaction—phenol degradation—used as a model in photocatalytic oxidation studies.<sup>29-33</sup>

## Experimental

The setup of the experimental apparatus, illustrated in Figure 1a, mainly consists of a radiation source and a photoreactor. An illuminator–collimator (Oriell Corporation, Stratford, CT), equipped with a 1000-W high-pressure Hg lamp (L5173 Hanovia) and a monochromator (Oriell model 7240), allowed us to carry out runs at fixed wavelength ( $370$  or  $310 \pm 2$  nm). A water filter was present in the illuminator so that IR radiation was cut off. The photoreactor consisted of two cylindrical vessels (ID 58 mm) of quartz glass, vertically positioned one

on the top of the other; the external surfaces of both vessels were covered by mirror-polished aluminum sheets. The upper vessels contained the aqueous  $\text{TiO}_2$  dispersion and the lower one the actinometric solution. The  $\text{TiO}_2$  dispersion was directly irradiated from the circular top surface of the upper vessel.

The actinometric solution was a ferrioxalate one,<sup>34</sup> appropriate for measuring the 370- or 310-nm photons; the volume of the actinometric solution was always 40  $\text{cm}^3$ . The absorbance of the actinometric samples was measured at  $\lambda = 510$  nm by using a Shimadzu UV2401 spectrophotometer. The temperature of the whole system was about 308 K for all experiments.

The following commercial  $\text{TiO}_2$  samples were used: P25 Degussa (80% anatase, 20% rutile), Merck (100% anatase), and Tioxide A (100% anatase). BET (Brunauer–Emmett–Teller) specific surface areas (SSA) of the solids were measured by using a Micromeritics Flow Sorb 2100 apparatus.

Particle sizes ( $d_p$ ) were determined by scanning electron microscopy (SEM; Philips ESEM SE 30). The samples were sonicated in water for nearly 30 min and the obtained dispersions were sprayed onto metal stubs, dried in air at ambient temperature, and covered with a thin layer of gold. The particles dispersed in water form aggregates, the sizes of which ( $d_a$ ) were measured in situ by using a Malvern light-scattering laser (model Mastersizer 2000).

Two different series of experimental runs were carried out: the former were performed to determine the transmitted photon flow as a function of the catalyst mass. These runs lasted 120 s (at 370 nm) or 180 s (at 310 nm) and were carried out by using a suspension volume of 100  $\text{cm}^3$ . The transmittance measurements were carried out at  $\text{pH} \approx 6.3$ , a value near to the zero point charge of  $\text{TiO}_2$ . The latter series of runs allowed us to determine the values of the rate constants of the photocatalytic oxidation of phenol. The photoreactivity tests were carried out at the same experimental conditions used for the transmittance measurements by using the amount of catalyst for which the transmitted photon flow was about 10% of the incident one. This amount, dependent on the  $\text{TiO}_2$  sample, was the highest one used for the transmittance measurements; in this way it was guaranteed for all the measurements that radiation reached the whole suspension. The initial phenol concentration was about 20 ppm; suspension samples of 4  $\text{cm}^3$  were withdrawn approximately every 30 or 60 min for phenol quantitative determination through a standard colorimetric method.<sup>35</sup> After each withdrawal the vessel containing the suspension was raised to restore the initial distance of free surface from the collimating lenses.

## Models for Determination of Optical Parameters

The optical parameters of an irradiated scattering medium may be evaluated by solving the RTE, which expresses the radiation intensity balance at a fixed wavelength  $\lambda$  as<sup>10</sup>

$$\begin{aligned} \text{Spatial intensity variation} + \text{absorption} + \text{out-scattering} \\ = \text{emission} + \text{in-scattering} \quad (1) \end{aligned}$$

indicating that the intensity of radiation of wavelength  $\lambda$ , by traveling a certain distance in the direction of radiation propagation in the medium, is diminished as a result of both

absorption and scattering, the latter phenomenon taking energy away from the propagation direction into all other directions. The sum of the absorption and scattering coefficients is the extinction coefficient of the medium and characterizes the attenuation of radiation. There is also an increase of intensity arising from emission and scattering of radiation from other directions into the direction of radiation propagation. The in-scattering term contains the so-called phase function, which gives the probability of scattering between the direction of radiation propagation and the other directions.

The analytical expression of the RTE involves an integro-differential equation, the solution of which is a very difficult task. It is therefore necessary to simplify the problem. One type of approach is based on the following assumptions:

- (1) The participating medium is constituted by parallel layers of a rectangular space where the incident radiation impinges perpendicularly from the collimated beam.
- (2) The layer is subjected to diffuse radiation.
- (3) The scattering and absorption coefficients are properties of a continuum irradiated layer (assumption of a pseudo-homogeneous medium<sup>14</sup>).
- (4) The cosine–Lambert law holds, corresponding to the hypothesis of isotropic distribution of scattering, neglecting the regular reflection; in this case<sup>20</sup> the phase function can be made equal to one.
- (5) The particles of the participant layer are randomly distributed and their size is smaller than the thickness of the layer.
- (6) The size parameter  $\tau$  satisfies the following inequality<sup>36</sup>:

$$\tau \equiv \frac{\pi D_p n_\lambda}{\lambda} > 5$$

in which  $D_p$  is the average particle diameter,  $\lambda$  is the radiation wavelength, and  $n_\lambda$  is the refractive index of the particle (for titanium dioxide<sup>32</sup>  $n_\lambda \approx 2.4$ ); the fulfillment of this condition allows us to model the light scattering by geometrical optics.

- (7) The emission term is negligible as a result of the low temperature prevailing in the participating medium.

Under these assumptions, a very simple approach to the RTE is the Schuster–Schwarzschild approximation,<sup>37</sup> which consists in dividing the radiation field into two oppositely directed radiation fluxes. By indicating with  $I$  the radiation flux in the positive direction perpendicular to the boundary plane of the layer and with  $J$  that in the opposite direction resulting from scattering, the radiation transfer equation generates two differential equations:

$$-\frac{dI}{dx} = (k + s)I - sJ \quad (2)$$

$$+\frac{dJ}{dx} = (k + s)J - sI \quad (3)$$

in which  $x$  is the coordinate along which light propagation occurs, and  $k$  and  $s$  are the absorption and scattering coefficients, respectively.

Several solutions have been proposed for these equations. The most generally accepted in the field of diffuse reflectance is the hyperbolic solution of Kubelka–Munk,<sup>38</sup> which reads

$$T = \frac{\sqrt{\left(1 + \frac{K}{S}\right)^2 - 1}}{\left(1 + \frac{K}{S}\right) \sinh\left[Sx \sqrt{\left(1 + \frac{K}{S}\right)^2 - 1}\right] + \sqrt{\left(1 + \frac{K}{S}\right)^2 - 1} \cosh\left[Sx \sqrt{\left(1 + \frac{K}{S}\right)^2 - 1}\right]} \quad (4)$$

in which  $T$  is the medium transmittance (the ratio between the transmitted photon flow to the incident one),  $K = 2k$ ,  $S = 2s$ , and  $x$  is the thickness of the participating medium. To apply this equation to model the experimental transmittance data, further manipulations are needed, as shown below: these allow determination of the scattering ( $s$ ) and absorption ( $k$ ) coefficients of the suspensions.

A monodirectional and monodimensional model has been recently used<sup>39</sup> to solve the RTE by two simplified approaches: a Kubelka–Munk type of solution and a DOM. The second approach was also validated with a more elaborated bidirectional and two-dimensional DOM model. It was found that, despite its simplicity and restrictions, the Kubelka–Munk method is able to yield fair order-of-magnitude estimates of the spectral optical properties of the used catalysts. On this ground it is important to outline that the  $s$  and  $k$  values obtained with the Kubelka–Munk method may be confidently used only for comparing different photocatalytic systems investigated under the same experimental conditions.

## Quantum Yield Determination

For heterogeneous photocatalytic systems in a kinetic regime the reaction rate  $r$  is a function of reactant and product concentration (through the site fractional coverage  $\theta$ ) and of the rate of photon absorption  $e_{\lambda}^a$ :

$$r = \varphi_{\lambda} f(e_{\lambda}^a, \theta) \quad (5)$$

The proportionality constant  $\varphi_{\lambda}$ , known as the *quantum yield*, is a function of wavelength. In the case in which the suspension is irradiated by radiation with  $\Delta\lambda$  range, the average value of  $\varphi_{\lambda}$  must be used for the whole range of  $\Delta\lambda$  where the catalyst absorbs radiation; in this case the  $\varphi_{\lambda}$  average value is called *quantum efficiency*. The quantity  $e_{\lambda}^a$ , which is the local volumetric rate of photon absorption, is a function of wavelength and the concentration of all the radiation absorbing species. It can be calculated once a solution of the RTE gives for any point of the medium the value of radiation intensity traveling along any direction  $\omega$  with a wavelength  $\lambda$ ,  $I_{\lambda\omega}$ , according to

$$e_{\lambda}^a = k_{\lambda} \int_{4\pi} I_{\lambda\omega} d\omega \quad (6)$$

To compare the performances of different photocatalytic systems it has been proposed<sup>24,25</sup> that the following two parameters be determined: the photon absorption rate by the catalyst (parc), defined as the ratio between the volumetric rate of photon absorption and the catalyst surface area per unit volume,

$$\text{parc} = \frac{\text{absorbed photons}}{(\text{time}) \cdot (\text{surface area})} \quad \left( \frac{\text{einstein}}{\text{s} \cdot \text{m}^2} \right) \quad (7)$$

and the intrinsic reaction rate (irr), defined as the ratio between the reacted molecules per unit volume and time and the catalyst surface area per unit volume,

$$\text{irr} = \frac{\text{reacted molecules}}{(\text{time}) \cdot (\text{surface area})} \quad \left( \frac{\text{mol}}{\text{s} \cdot \text{m}^2} \right) \quad (8)$$

Knowledge of parc and irr allows us to determine the quantum yield ( $\varphi$ ) for monochromatic radiation:

$$\varphi = \frac{\text{reacted molecules}}{\text{absorbed photons}} = \frac{\text{irr}}{\text{parc}} \quad (9)$$

In the absence of a solution to the RTE, the photon flow absorbed by the photocatalyst particles can be estimated by using a method reported in the literature.<sup>27</sup> The following macroscopic energy balance can be performed on the whole suspension under the assumption that it does not lose radiation through the lateral wall (see Figure 1b):

$$\Phi_i = \Phi_r + \Phi_a + \Phi_t \quad (10)$$

in which  $\Phi_i$  represents the incident photon flow,  $\Phi_r$  is the backward scattered photon flow,  $\Phi_a$  is the absorbed photon flow, and  $\Phi_t$  is the transmitted photon flow.

Experimentally, it was found<sup>25,26</sup> that the dependency of transmitted photon flow on mass of catalyst follows an apparent LBL, when the mass of catalyst is higher than a threshold value:

$$\Phi_t = \Phi' \exp(-Em_{\text{cat}}) \quad (11)$$

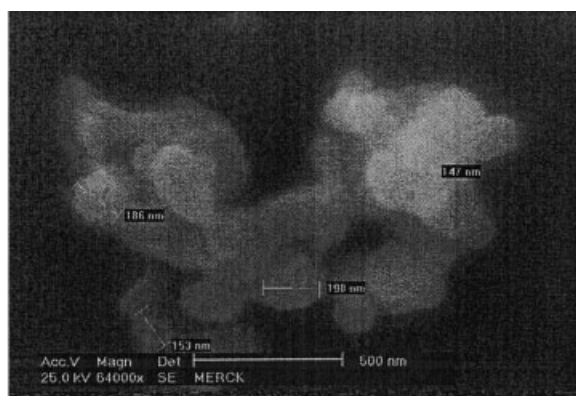
in which  $\Phi'$  is a constant whose value is  $\leq \Phi_i$ ,  $E$  is the Napierian extinction coefficient,<sup>33</sup> and  $m_{\text{cat}}$  is the mass of catalyst.

By substituting Eq. 11 into Eq. 10 and by considering that the absorbed photon flow is a function of the mass of catalyst, the resulting energy balance, evaluated for  $m_{\text{cat}} = 0$ , allows determination of  $\Phi_r$ :

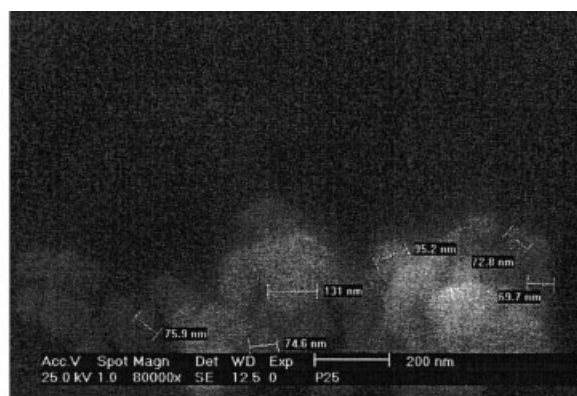
$$\Phi_r = \Phi_i - \Phi' \quad (12)$$

It is important to stress that Eq. 12 is obtained from a photon flow balance valid only if the mass of catalyst of the suspension is above a threshold value. In other words,  $\Phi_r$  represents the photon flow backward reflected by a medium so optically thick





(A)



(B)



(C)

**Figure 2. SEM microphotographs of different titanium dioxide samples.**

(A) Merck; (B) Degussa P25; (C) Tioxide A.

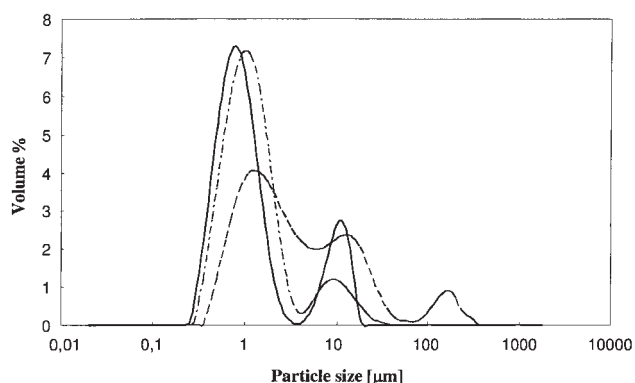


**Figure 3. Particle size distribution curves of different titanium dioxide samples.**

(---) Merck; (-.-) Degussa P25; (—) Tioxide A.

that the reflectance may be hypothesized to be independent of the medium depth, that is, of the catalyst mass.

## Results and Discussion

Figure 2 shows SEM microphotographs of the titanium dioxide samples, for which it was possible to measure the size of the primary particles, whereas Figure 3 shows the distribution curves of the sizes of the agglomerates. It can be noticed that, at a pH close to the zero point charge of titanium dioxide, the charge

**Table 1. Values of Primary Particle Size, Mean Size of the Agglomerates, Specific Surface Area, and Size Parameter ( $\tau$ ) of Photocatalysts Used**

Catalyst	$d_p$ (nm)	$d_a$ ( $\mu\text{m}$ )	SSA ( $\text{m}^2 \text{g}^{-1}$ )	$\tau$
Degussa P25	$60 \div 130$	$1.67 \div 16.45$	50	$>34.0$
Merck	$100 \div 200$	$1.10 \div 12.00$	10	$>22.4$
Tioxide A	$150 \div 200$	$0.78 \div 10.00$	8	$>14.5$

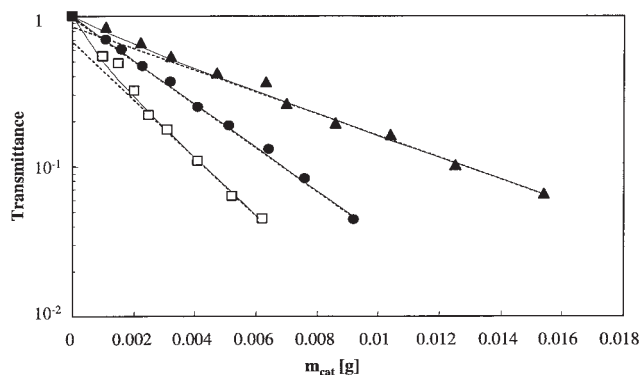


**Figure 4. Transmittance values vs. the amount of solid,  $m_{\text{cat}}$ , in the presence of monochromatic radiation at 370 nm for different  $\text{TiO}_2$  samples.**

(□) Degussa P25; (●) Tioxide A; (▲) Merck. The continuous lines through the data represent the Kubelka-Munk hyperbolic model (Eq. 16) and the broken lines represent the phenomenological relationship (Eq. 20).

on the particles is decreased, which leads to particle aggregation. Indeed, in Figure 3 both the size of the primary aggregates (higher peaks at lower particle size) and the size of the large aggregates formed in the destabilized slurry can be determined. The values of the primary particle size and the mean size of the aggregate are reported in Table 1 together with the specific surface areas (SSA) and the size parameters ( $\tau$ ) calculated for the lowest agglomerate size and the highest wavelength.

Preliminary experiments carried out with the same amount of solid suspended in different water volumes showed the same values of transmittance, indicating that only the total mass of semiconductor particles influences the optical behavior of the system, and not its volume concentration. This important feature may be accounted for, as shown below. On this basis, transmittance measurements were carried out with a constant suspension volume by varying the mass of catalyst; therefore the results are reported as transmittance vs. the catalyst mass.

The values of transmittance were calculated as the ratio between the transmitted photon flow, determined with the photoreactor filled with the suspension, and the incident flow determined with the photoreactor filled with distilled water.

Figure 4 shows the values of transmittance vs.  $m_{\text{cat}}$  in the presence of monochromatic radiation at 370 nm; the incident photon flow was  $7.82 \times 10^{-8} \text{ einstein} \cdot \text{s}^{-1}$ .

Figure 5 shows the values of transmittance vs.  $m_{\text{cat}}$  in the presence of monochromatic radiation at 310 nm; the incident photon flow was  $4.77 \times 10^{-8} \text{ einstein} \cdot \text{s}^{-1}$ .

With respect to  $\text{TiO}_2$  P25 Degussa, it was not possible to carry out transmittance measurements at 310 nm because the radiation was almost quantitatively absorbed even in the pres-

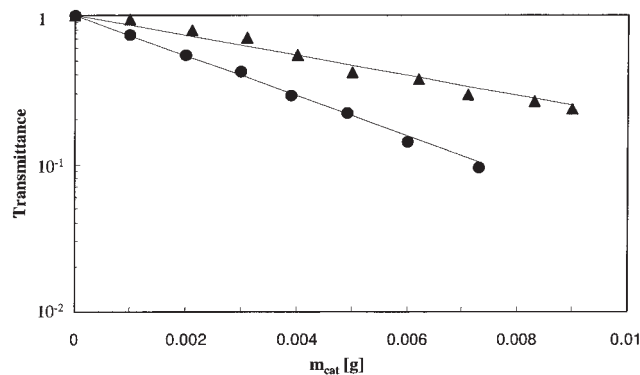


**Figure 5. Transmittance values vs. the amount of solid,  $m_{\text{cat}}$ , in the presence of monochromatic radiation at 310 nm for different  $\text{TiO}_2$  samples.**

Symbols and lines as in Figure 4.

ence of a very low amount of solid. For high solid amounts (optically thick medium) the transmitted photon flow was under the detection limit, indicating that only an (unknown) aliquot of the suspension was reached by radiation.

Equation 4 gives the transmittance  $T$  as a function of  $x$ , the thickness of the participating medium,<sup>38</sup> whereas it is desirable to have Eq. 4 as a function of the mass of catalyst  $m_{\text{cat}}$ . To do so,  $x$  is expressed as

$$x = \frac{m_{\text{cat}}}{Ac_{\text{cat}}} \quad (13)$$

where  $A$  is the cross section of the photoreactor ( $26.42 \text{ cm}^2$ ) and  $c_{\text{cat}}$  is the catalyst concentration of the suspension.

The scattering ( $s$ ) and absorption ( $k$ ) coefficients also depend on particle concentration. It is usually assumed<sup>38</sup> that there is direct proportionality between both optical parameters and the concentration:

$$s = s^* \cdot c_{\text{cat}} \quad k = k^* \cdot c_{\text{cat}} \quad (14)$$

where  $s^*$  and  $k^*$  are the scattering and absorption coefficients, respectively, per unit concentration, which depend only on wavelength. In other applications of the Kubelka-Munk theory, such as when the absorbing/scattering particles also carry transition metal ions capable of further absorption, different assumptions are made.<sup>38</sup>

By considering Eqs. 13, 14, and 4, the following equation is obtained:

$$T = \frac{\sqrt{\left(1 + \frac{k^*}{s^*}\right)^2 - 1}}{\left(1 + \frac{k^*}{s^*}\right) \sinh\left[\frac{2s^*m_{\text{cat}}}{A} \sqrt{\left(1 + \frac{k^*}{s^*}\right)^2 - 1}\right] + \sqrt{\left(1 + \frac{k^*}{s^*}\right)^2 - 1} \cosh\left[\frac{2s^*m_{\text{cat}}}{A} \sqrt{\left(1 + \frac{k^*}{s^*}\right)^2 - 1}\right]} \quad (15)$$

**Table 2. Values of  $s^*$  and  $k^*$  for the Various  $\text{TiO}_2$  Samples under Different Irradiation Conditions\***

Catalyst	Hyperbolic Equation (Eq. 16)		Exponential Equation (Eq. 20)	
	$s^*$ (cm <sup>2</sup> /g)	$k^*$ (cm <sup>2</sup> /g)	$s^*$ (cm <sup>2</sup> /g)	$k^*$ (cm <sup>2</sup> /g)
Monochromatic radiation at 370 nm				
P25 Degussa	10000	1600	10200	1550
Merck	2165	910	2181	892
Tioxide A	900	3600	686	3657
Monochromatic radiation at 310 nm				
Merck	(0.01)	2110	—	2140
Tioxide A	(0.29)	4245	—	4372

\*The figures in parentheses can be considered negligible.

Equation 15 may actually be rewritten in a much more readable form:

$$T = \frac{(1 - R_\infty^2) \exp\left(-b \frac{2s^*m_{\text{cat}}}{A}\right)}{1 - R_\infty^2 \exp\left(-2b \frac{2s^*m_{\text{cat}}}{A}\right)} \quad (16)$$

where  $R_\infty$  is the so-called diffuse reflectance of the sample and is a function of only the  $k^*/s^*$  ratio (the Kubelka–Munk function for isotropic scattering):

$$R_\infty = 1 + \frac{k^*}{s^*} - \sqrt{\left(\frac{k^*}{s^*}\right)^2 + 2 \frac{k^*}{s^*}} \quad (17)$$

and  $b$  is defined as

$$b = \sqrt{\left(1 + \frac{k^*}{s^*}\right)^2 - 1} \quad (18)$$

Equation 16 readily accounts for the form of the curves in Figure 4. Moreover, as shown later, it also accounts for the behavior of optically thick media. The spectral optical coefficients  $k^*$  and  $s^*$  were determined by using the nonlinear fitting algorithm of *Mathematica* software (Wolfram Research, Champaign, IL).

Table 2 reports the values of  $s^*$  and  $k^*$  so obtained for the various  $\text{TiO}_2$  samples under different irradiation conditions. The continuous curves in Figures 4 and 5 represent the model expressed in Eq. 16. A very good fitting of the hyperbolic model of Kubelka and Munk to the experimental data may be noted for all of the samples.

The optical coefficients values reported in Table 2 (hyperbolic equation) show that only few samples exhibit significant

scattering and, consequently, the scattering contribution is not always necessary to verify the efficiency of the system. By changing the irradiation from 370 to 310 nm, the scattering coefficient decreases and the absorption coefficient increases.<sup>11</sup>

For a participating optically thick medium, that is, in our case at high values of catalyst mass, Eq. 16 may be approximated by the following expression:

$$T = (1 - R_\infty^2) \exp\left(-b \frac{2s^*m_{\text{cat}}}{A}\right) \quad (19)$$

Equation 19 shows that there is an exponential relationship between the transmittance and the mass of catalyst. The same dependency is shown by the phenomenological Eq. 11 in which the  $\Phi'$  constant and the Napierian extinction coefficient appear. In fact, by dividing Eq. 11 for the incident photon flow, the following relationship is obtained:

$$\frac{\Phi_i}{\Phi_i} \equiv T = \frac{\Phi'}{\Phi_i} \exp(-Em_{\text{cat}}) \quad (20)$$

By comparing Eq. 19 with Eq. 20 the following identities may be deduced:

$$\Phi' = \Phi_i(1 - R_\infty^2) \quad (21)$$

$$E = 2 \frac{s^*}{A} \sqrt{\left(1 + \frac{k^*}{s^*}\right)^2 - 1} \quad (22)$$

On this ground the transmittance data at high values of catalyst mass have been fitted to Eq. 20 and the best values of  $\Phi'$  and  $E$  have been determined with *Mathematica* software by a linear regression analysis using a least-squares best-fitting procedure. Table 3 reports the  $\Phi'$  and  $E$  values obtained under different irradiation conditions.

The values of  $\Phi'$  and  $E$  of Table 3 have been used to determine the values of  $s^*$  and  $k^*$  by means of Eqs. 21 and 22. In fact by knowing  $\Phi'$  Eq. 21 gives the  $R_\infty$  value, which through Eq. 17 furnishes the value of the  $k^*/s^*$  ratio. By inserting the known values of  $E$  and  $k^*/s^*$  in Eq. 22 the value of  $s^*$  may be determined and therefore that of  $k^*$ . The values of  $s^*$  and  $k^*$  obtained by means of this procedure, which starts by the values of  $\Phi'$  and  $E$ , are reported in Table 2 (exponential equation, Eq. 20); it is useful to report that these values were used as starting guesses in the nonlinear fitting procedure applied to Eq. 16. The data of Table 2 allow one to compare the values of  $s^*$  and  $k^*$  obtained from the phenomenological rela-

**Table 3. Values of  $\Phi'$ ,  $E$ ,  $\Phi_r$ ,  $\Phi_i$ , and  $\Phi_a$  for the Various  $\text{TiO}_2$  Samples under Different Irradiation Conditions**

Catalyst	$\Phi' \times 10^8$ (einstein/s)	$E$ (g <sup>-1</sup> )	$\Phi_r \times 10^8$ (einstein/s)	$\Phi_i \times 10^8$ (einstein/s)	$\Phi_a \times 10^8$ (einstein/s)
Monochromatic radiation at 370 nm: $\Phi_i = 7.82 \times 10^{-8}$ einstein/s					
P25 Degussa	5.311	440	2.642	0.352	4.824
Merck	6.464	164	1.354	0.521	5.943
Tioxide A	7.765	325	0.053	0.391	7.370
Monochromatic radiation at 310 nm: $\Phi_i = 4.77 \times 10^{-8}$ einstein/s					
Merck	4.766	162	—	1.181	3.585
Tioxide A	4.766	331	—	0.454	4.312

tionship with those obtained from the hyperbolic Kubelka–Munk model (Eq. 16). It may be noted that negligible scattering coefficients were determined for samples with negligible reflected photon flows, thus confirming the validity of the method previously reported.<sup>23–27</sup> On this ground it may be concluded that the phenomenological relationship–like Lambert–Beer law (Eq. 11) is only an asymptotic solution of the Kubelka–Munk model and that it is valid for describing the dependency of transmitted photon flow on the catalyst mass under the condition that the suspension is optically thick. This condition is fulfilled when the following inequality is satisfied (see Eq. 16):

$$m_{\text{cat}} > \frac{A}{4bs^*} \quad (23)$$

By introducing Eqs. 18 and 22 in Eq. 23 we obtain

$$m_{\text{cat}} > \frac{1}{2E} \quad (24)$$

In conclusion, once the value of  $E$  is obtained, it must verify that masses of catalyst used for obtaining the experimental data of transmitted photon flow satisfy Eq. 24; in this case the photon flow balance expressed by Eq. 10 can be used to determine the absorbed photon flow.

The calculated absorption coefficients are of the same order of magnitude of data found in the literature, whereas the scattering coefficients are lower.<sup>33,40</sup> It is known that at neutral pH titanium dioxide tends to agglomerate<sup>41</sup>; in fact  $\text{TiO}_2$  is not dispersed in the water phase as primary particles but rather as solid  $\text{TiO}_2$  aggregates.<sup>14</sup> Degussa P25, Merck, and Tioxide A form agglomerates ranging between 1.1 and 16.5  $\mu\text{m}$ , although for all of them the primary particle sizes are  $<200$  nm (see Table 1). The catalyst concentration also affects the agglomeration, which increases by increasing the concentration. In this case the agglomeration facilitates the penetration of the photons through the medium and accordingly the absorption and scattering coefficients decrease. It is reasonable, anyway, to hypothesize that the different degree of agglomeration depending on pH and concentration leads to uncertainties in the optical properties of the  $\text{TiO}_2$  catalyst.<sup>42</sup>

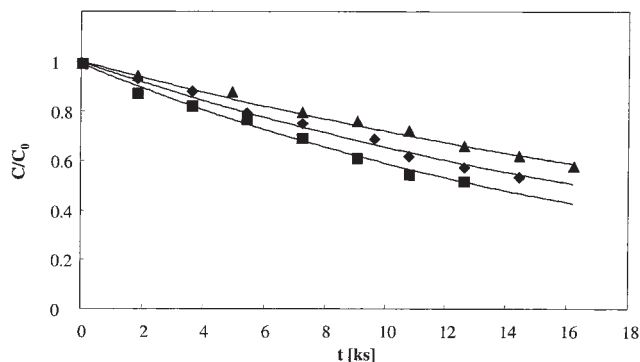


**Figure 6. Phenol concentration over initial phenol concentration  $C/C_0$  vs. time  $t$ , for photoreactivity runs carried out at 370 nm.**

(◆) Degussa P25; (■) Merck; (▲) Tioxide A.

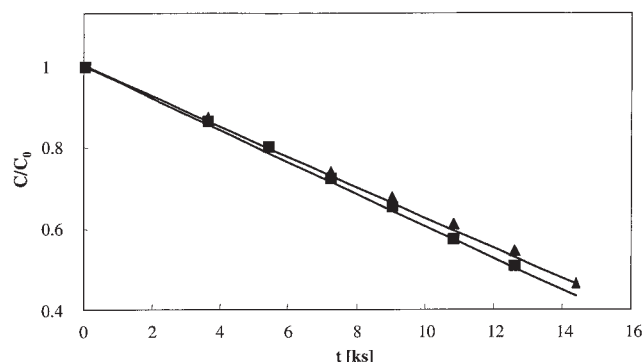


**Figure 7. Phenol concentration over initial phenol concentration  $C/C_0$  vs. time  $t$ , for photoreactivity runs carried out at 310 nm.**

(■) Merck; (▲) Tioxide A.

To determine the quantum yield values the phenol degradation rate was determined under the same irradiation conditions used for transmittance measurements.

The rate of phenol photocatalytic degradation in oxygenated suspensions is reported<sup>29–32</sup> to obey a second-order kinetics because it depends on coverages by oxygen and phenol that adsorb on different types of sites existing on the irradiated catalyst surface. The surface reaction rate  $r_s$  is written in terms of Langmuir–Hinshelwood kinetics as

$$r_s = -\frac{1}{S} \frac{dN}{dt} = k''\theta_{\text{Ox}}\theta_{\text{PHEN}} \quad (25)$$

in which  $N$  indicates the phenol moles present in the liquid phase;  $t$  is the reaction time;  $S$  is the catalyst surface area;  $k''$  is the surface second-order rate constant; and  $\theta_{\text{Ox}}$  and  $\theta_{\text{PHEN}}$  are the fractional sites coverages by oxygen and phenol, respectively. Given that all the experiments of this work were carried out in a stirred batch reactor in contact with atmospheric air, the  $\theta_{\text{Ox}}$  term does not change during the occurrence of phenol photooxidation. Therefore in Eq. 25 the  $k''\theta_{\text{Ox}}$  term can be substituted by  $k'$ , which is the surface pseudo-first-order rate constant.

The fractional site coverage by phenol ( $\theta_{\text{PHEN}}$ ) is given by the Langmuir relationship:

$$\theta_{\text{PHEN}} = \frac{KC}{1 + KC} \quad (26)$$

**Table 4. Observed Rate Constants and Moles of Reacted Molecules during the Irradiation Time Used for the Transmitted Light Measurements**

Photocatalyst	Observed Rate Constants	Reacted Molecules (mol)
Monochromatic radiation at 370 nm: $k'K [=] \text{ m s}^{-1}$		
P25 Degussa	$1.5 \times 10^{-8}$	$1.1 \times 10^{-7}$
Merck	$3.4 \times 10^{-8}$	$1.4 \times 10^{-7}$
Tioxide A	$4.7 \times 10^{-8}$	$0.9 \times 10^{-7}$
Monochromatic radiation at 310 nm: $k' [=] \text{ mol m}^{-2} \text{ s}^{-1}$		
Merck	$9.55 \times 10^{-6}$	$1.6 \times 10^{-7}$
Tioxide A	$1.31 \times 10^{-5}$	$1.4 \times 10^{-7}$



**Table 5. Quantum Yield ( $\varphi$ ) Values Determined for All the Experimental Conditions Used**

Catalyst	$\varphi$ (%)
Monochromatic radiation at 370 nm ( $t = 120$ s)	
P25 Degussa	1.90
Merck	1.96
Tioxide A	1.02
Monochromatic radiation at 310 nm ( $t = 180$ s)	
Merck	2.48
Tioxide A	1.80

in which  $C$  is the phenol concentration in the solution and  $K$  is the adsorption equilibrium constant. By substituting Eq. 26 in Eq. 25 and by considering that the phenol concentration was the parameter experimentally measured, the pseudo-first-order rate equation assumes the following form:

$$r_s = -\frac{V}{S} \frac{dC}{dt} = k' \frac{KC}{1 + KC} \quad (27)$$

The runs carried out by using monochromatic radiation at 370 nm indicated that phenol degradation rate follows a first-order kinetics for all of the catalysts (Figure 6), whereas the experiments carried out under monochromatic radiations at 310 nm showed a zero-order kinetics (Figure 7). Depending on the  $KC$  group value, Eq. 27 may give first- or zero-order kinetics; in fact for  $KC \ll 1$ , Eq. 27 gives  $r_s = k'KC$ , whereas for  $KC \gg 1$ ,  $r_s = k'$ . The finding at equal  $C$  values of a first-order kinetics at  $\lambda = 370$  nm and of a zero order at  $\lambda = 310$  may be explained by considering that the increase of radiation energy (equivalent to an increase of temperature) increases the  $K$  value.

By integrating the first- and zero-order rate equations and by fitting the resulting equations to the experimental  $C-t$  data, the values of the  $k'K$  group and  $k'$  have been obtained. Table 4 reports the figures of those constants for all the photocatalysts under the different irradiation conditions and the number of molecules reacted in the time spent for measuring the transmitted photon flow. The quantum yield ( $\varphi$ ) values, determined by using Eq. 9, are reported in Table 5.

Through comparison, the values of  $\varphi$  were found to increase by decreasing the wavelength of the irradiating beam. This behavior can be explained by considering the values of radiation absorption coefficients (Table 2) and the number of reacted molecules (Table 4). The results suggest that the coverage of active sites increases by increasing the photon energy. Indeed, because the absorption coefficient values also increase (see Table 2), it can then be hypothesized that there is a parallel increase of the number of sites available for the occurrence of photoreaction and quantum yield.

## Acknowledgments

V. Augugliaro expresses thanks to Rafael González Pérez for the invaluable help given in the course of this work. M. Addamo thanks Tioxide and Degussa for generously supplying some  $\text{TiO}_2$  samples. Financial support from the Italian Ministry of Education, University and Research is gratefully acknowledged.

## Literature Cited

- Schiavello M, ed. *Photoelectrochemistry, Photocatalysis and Photoreactors. Fundamentals and Developments*. Dordrecht, The Netherlands: Reidel; 1985.
- Schiavello M, ed. *Photocatalysis and Environment. Trends and Applications*. New York, NY: Wiley; 1989.
- Serpone N, Pelizzetti E, eds. *Photocatalysis. Fundamentals and Applications*. New York, NY: Wiley; 1989.
- Childs LP, Ollis DF. Is photocatalysis catalytic? *J Catal*. 1988;66:383-390.
- H. Kisch. What is photocatalysis? In: Serpone N, Pelizzetti E, eds. *Photocatalysis. Fundamentals and Applications*. New York, NY: Wiley; 1989:1-8.
- Palmisano L, Augugliaro V, Campostri R, Schiavello M. A proposal for the quantitative assessment of heterogeneous photocatalytic processes. *J Catal*. 1993;143:149-154.
- Augugliaro V, Schiavello M, Palmisano L. Rate of photon absorption and turnover number: Two parameters for the comparison of heterogeneous photocatalytic systems in a quantitative way. *Coord Chem Rev*. 1993;125:173-182.
- Serpone N, Terzian R, Lawless D, Kennepohl P, Sauve G. On the usage of turnover numbers and quantum yields in heterogeneous photocatalysis. *J Photochem Photobiol A Chem*. 1993;73:11-16.
- Brandi RJ, Alfano OM, Cassano AE. Evaluation of radiation absorption in slurry photocatalytic reactors. 1. Assessment of methods in use and new proposal. *Environ Sci Technol*. 2000;34:2623-2630.
- Cassano AE, Alfano OM. Reaction engineering of suspended solid heterogeneous photocatalytic reactors. *Catal Today*. 2000;58:167-197.
- Satuf ML, Brandi RJ, Cassano AE, Alfano OM. Experimental method to evaluate the optical properties of aqueous titanium dioxide suspensions. *Ind Eng Chem Res*. 2005;44:6643-6649.
- Martin CA, Sgalari G, Santarelli F. Photocatalytic processes using solar radiation. Modeling of photodegradation of contaminants in polluted waters. *Ind Eng Chem Res*. 1999;38:2940-2946.
- Arancibia-Bulnes CA, Bandala ER, Estrada CA. Radiation absorption and rate constants for carbaryl photocatalytic degradation in a solar collector. *Catal Today*. 2002;76:149-159.
- Alfano OM, Cabrera MI, Cassano AE. Modeling of light scattering in photochemical reactors. *Chem Eng Sci*. 1994;49:5327-5346.
- Pasquali M, Santarelli F, Porter JF, Yue PL. Radiative transfer in photocatalytic systems. *AIChE J*. 1996;42:532-537.
- Arancibia-Bulnes CA, Ruiz-Suárez JC. Average path-length parameter of diffuse light in scattering media. *Appl Optics*. 1999;38:1877-1883.
- Romero RL, Alfano OM, Cassano AE. Cylindrical photocatalytic reactors. Radiation absorption and scattering effects produced by suspended fine particles in an annular space. *Ind Eng Chem Res*. 1997;36:3094-3109.
- Sgalari G, Camera-Roda G, Santarelli F. Discrete ordinate method in the analysis of radiative transfer in photocatalytically reacting media. *Int Commun Heat Mass Transfer*. 1998;5:651-660.
- Martin CA, Camera-Roda G, Santarelli F. Effective design of photocatalytic reactors: Influence of radiative transfer on their performance. *Catal Today*. 1999;48:307-313.
- Brandi RJ, Alfano OM, Cassano AE. Rigorous model and experimental verification of the radiation field in a flat solar collector simulator employed for photocatalytic reactions. *Chem Eng Sci*. 1999;54:2817-2827.
- Li HY, Özisik MN. Simultaneous conduction and radiation in a two-dimensional participating cylinder with anisotropic scattering. *J Quant Spectrosc Radiat Transfer*. 1991;46:393-404.
- Brucato A, Rizzuti L. Simplified modeling of radiant fields in heterogeneous photoreactors. 1. Case of zero reflectance. *Ind Eng Chem Res*. 1997;36:4740-4747.
- Augugliaro V, Palmisano L, Schiavello M. Photon absorption by aqueous  $\text{TiO}_2$  dispersion contained in a stirred photoreactor. *AIChE J*. 1991;37:1096-1100.
- Schiavello M, Augugliaro V, Palmisano L. An experimental method for the determination of the photon flow reflected and absorbed by aqueous dispersions containing polycrystalline solids in heterogeneous photocatalysis. *J Catal*. 1991;127:332-341.
- Augugliaro V, Loddo V, Palmisano L, Schiavello M. Performance of heterogeneous photocatalytic systems: Influence of operational vari-

- ables on photoactivity of aqueous suspension of  $\text{TiO}_2$ . *J Catal.* 1995; 153:32-40.
26. Augugliaro V, Loddo V, Palmisano L, Schiavello M. Heterogeneous photocatalytic systems: Influence of some operational variables on actual photons absorbed by aqueous dispersions of  $\text{TiO}_2$ . *Solar Energy Mater Solar Cells.* 1995;38:411-419.
  27. Augugliaro V, Loddo V, Palmisano L, Schiavello M. Bestimmung der quantenausbeute von heterogenen photokatalytischen systemen. Bestimmung des absorbierten und reflektierten photonenflusses in wäßrigen suspensionen von polykristallinem titandioxid. In: Wöhrle D, Tausch MW, Stohrer WD, eds. *Photochemie Konzepte, Methoden, Experimente*. Weinheim, Germany: Wiley-VCH; 1998:459-465.
  28. Martín CA, Baltanás MA, Cassano AE. Photocatalytic reactors I. Optical behavior of titanium oxide particulate suspensions. *J Photochem Photobiol A Chem.* 1993;76:199-208.
  29. Augugliaro V, Palmisano L, Sclafani A, Minero C, Pelizzetti E. Photocatalytic degradation of phenol in aqueous titanium dioxide dispersions. *Toxicol Environ Chem.* 1988;16:89-109.
  30. Augugliaro V, Davì E, Palmisano L, Schiavello M, Sclafani A. Influence of hydrogen peroxide on the kinetics of phenol photodegradation in aqueous titanium dioxide dispersion. *Appl Catal.* 1990;65:101-116.
  31. Wei T-Y, Wan C-C. Kinetics of photocatalytic oxidation of phenol on  $\text{TiO}_2$  surface. *J Photochem Photobiol A Chem.* 1992;69:241-249.
  32. Chen D, Ray AK. Photocatalytic kinetics of phenol and its derivatives over UV irradiated  $\text{TiO}_2$ . *Appl Catal B Environ.* 1999;23:143-157.
  33. Brandi RJ, Citroni MA, Alfano OM, Cassano AE. Absolute quantum yields in photocatalytic slurry reactors. *Chem Eng Sci.* 2003;58:979-985.
  34. Murov SL, ed. *Handbook of Photochemistry*. New York, NY: Marcel Dekker; 1973.
  35. Taras HJ, Greenberg AE, Hoak RD, Rand MC, eds. *Standard Methods for Examination of Water and Wastewater*. Washington, DC: American Public Health Association; 1971.
  36. Özisik MN. *Radiative Transfer and Interactions with Conduction and Convection*. New York, NY: Wiley; 1973.
  37. Modest MF. *Radiative Heat Transfer*. New York, NY: McGraw-Hill; 1993.
  38. Kortüm G. *Reflectance Spectroscopy: Principles, Methods, Applications*. New York, NY: Springer-Verlag; 1969.
  39. Pozzo RL, Brandi RJ, Giombi J-L, Baltanás MA, Cassano AE. Design of fluidized bed photoreactors: Optical properties of photocatalytic composites of titania CVD-coated onto quartz sand. *Chem Eng Sci.* 2005;60:2785-2794.
  40. Cabrera MI, Alfano OM, Cassano AE. Absorption and scattering coefficients of titanium dioxide particulate suspensions in water. *J Phys Chem.* 1996;100:20043-20050.
  41. Pirkanniemi K, Sillanpää M. Heterogeneous water phase catalysis as an environmental application: A review. *Chemosphere.* 2002;48:1047-1060.
  42. Yang Q, Ang PL, Ray MB, Pehkonen SO. Light distribution field in catalyst suspensions within an annular photoreactor. *Chem Eng Sci.* 2005;60:5255-5268.

Manuscript received Nov. 10, 2005, and revision received Mar. 23, 2006.